Journal of Applied Polymer Science

Effect of 1,3,5-Trialkyl-Benzenetricarboxylamide on the Crystallization of Poly(lactic acid)

Ting Wang, Yong Yang, Chuanzhi Zhang, Zhaobin Tang, Haining Na, Jin Zhu
Ningbo Key Laboratory of Polymer Materials, Polymers and Composites Division, Ningbo Institute of Material Technology and Engineering, Chinese Academy of Sciences, Ningbo, Zhejiang 315201, China
Correspondence to: J. Zhu (E-mail: jzhu@nimte.ac.cn)

ABSTRACT: A series of 1,3,5-trialkyl-benzenetricarboxylamides (BTA-Rs) with different side-chain lengths of *n*-alkyl are synthesized to use as nucleating agents of poly (lactic acid) (PLA). Crystallization rate of PLA is detailed discussed in nonisothermal melt-crystallization with addition of the synthesized nucleating agents. Among these BTA-Rs, BTA-n-butyl (BTA-nBu) shows the most excellent nucleation ability for PLA. The influences of BTA-nBu on the nonisothermal melt-crystallization and cold-crystallization from the glassy state, isothermal crystallization, crystalline structure, and spherulite morphology of PLA are investigated. It is found that 0.8 wt % is the optimal weight fraction of BTA-nBu to improve the crystallization of PLA. In the case of isothermal melt-crystallization from melt, the addition of BTA-nBu shortens the crystallization half-time and speeds up the crystallization rate of PLA with no discernible effect on the crystalline structure. Besides, BTA-nBu nucleated PLA exhibits smaller spherulites size and larger nucleation density than that of pure PLA. © 2013 Wiley Periodicals, Inc. J. Appl. Polym. Sci. 000: 000–000, 2013

KEYWORDS: crystallization; differential scanning calorimetry (DSC); morphology

Received 17 December 2012; accepted 4 March 2013; Published online 00 Month 2013
DOI: 10.1002/app.39308

INTRODUCTION

Poly(lactic acid) (PLA) is one of the widely studied biodegradable and biocompatible polymers derived from renewable resources, because many of its properties are equivalent or superior to those of some petroleum-based plastics, which makes it suitable for various applications.[1,2] Because of the expectable rise in the cost of nonrenewable petroleum-based plastics in the next decades, it will open a bright perspective for PLA application.[3] However, PLA usually exhibits a low crystallization rate and thus low crystallinity resulting in a difficult process by the traditional injection molding. Numerous studies were carried out to find a way to improve the crystallization rate of PLA for example minimizing the amount of D-lactide isomers in L-lactide,[4,5] adding nucleating agent,[6–8] adding plasticizer,[9–11] and optimizing the molding conditions.[12–14] Essentially, the most useful and effective way is recognized as adding nucleating agent in PLA.

Although a great number of investigations has been related to inorganic nucleating agents of PLA,[15–23] the ultimate physical properties of the PLA is rather low owing to the poor compatibility between PLA and nucleating agents.[24] In the contrary, organic nucleating agent can exhibit good compatibility and solubility with PLA. Crystallization rate of PLA is effectively increased by adding organic nucleating agent as reported.[24–30] As we know, substituted 1,3,5-benzenetrisamides are superior organic nucleating agents with excellent thermal and chemical stability. They have been extensively used as a highly effective nucleating agent for isotactic polypropylene (i-PP).[31–35] Recently, some kinds of 1,3,5-benzenetricarboxylamide (BTA) derivatives were used in PLA to improve the crystallization rate and crystallinity.[36–38] With the help of BTA-cyclohexyl (BTA-cHe), Bai et al.[36] succeeded in fabricating three different crystal morphologies of PLA. Song et al.[37] also reported the improvement of crystallization rate and increase of crystallinity by using BTA-cHe in PLA. Nakajima et al.[38] had ever paid attention to the solubility parameter of PLA and alkyl substituted BTA. It was concluded that BTA-*n*-alkyl showed a similar solubility parameter with PLA and thus the better compatibility. However, crystallization behavior of PLA/BTA-*n*-alkyl was not characterized in detail. It needs to develop a systematical research to understand the nucleation efficiency of *n*-alkyl substituted BTA in PLA.

In this article, a series of 1,3,5-trialkyl-benzenetricarboxylamides (BTA-Rs) with different side chain lengths of *n*-alkyl are prepared and used in PLA. The nonisothermal and isothermal crystallization are utilized to evaluate the crystallization of PLA nucleated by BTA-Rs, especially BTA-n-butyl (BTA-nBu) (Figure 1). Optimal amount and crystallization half-time of PLA/BTA-nBu blend are decided. Besides, the spherulitic

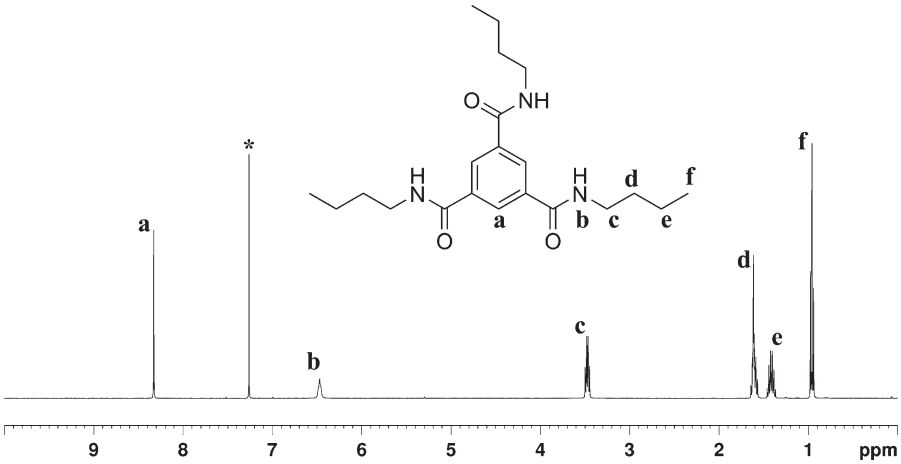

Figure 1. ^{1}H NMR spectra of BTA-n-butyl (BTA-nBu). [Asterisks denote the peak ascribed to $CDCl_3$ as solvent].

morphology and crystalline structures of nucleated PLA are also evaluated in detail.

EXPERIMENTAL

Materials

PLA (commercial grade 4032D, consist of ~2% D-LA) was purchased from Nature Works LLC. The weight-averaged molecular weight and polydispersity index are 207 and 1.74 kDa, respectively. Trimesoyl chloride, primary aliphatic amines, and lithium chloride were supplied by Aladdin Chemistry (Shanghai, China). Chemical reagents and solvents were obtained from Sinopharm Chemical Reagent (Shanghai, China).

Synthesis of BTA Derivatives

Five 1,3,5-trialkyl-benzenetricarboxylamides (BTA-Rs) with different n-alkyl moieties (R) as propyl (nPr), butyl (nBu), amyl (nAm), hexyl (nHe), and octyl (nOc) groups were synthesized in the same experimental procedures. The procedures were operated as follows: 0.035 mol primary aliphatic amines, 0.01 mol trimesoyl chloride, 7.4 mL pyridine, and 0.05 g lithium chloride were mixed and dissolved in 80 mL *N*,*N*-dimethylformamide (DMF). The reaction mixture was heated to 80°C and reacted for 3 h under stirring. Then the reaction mixture including BTA-R was cooled in air to room temperature then poured into 400 mL cold water with stirring to form insoluble floc. The floc was filtered off and dried at 85°C in vacuum oven for 12 h. The solid collected by filtration was dissolved and recrystallized by acetone for several times. Finally, white BTA-R crystals was formed and collected by filtration. BTA-Rs were dried in vacuum at 70°C overnight and then characterized by ^{1}H NMR, FTIR, and TGA/DSC. ^{1}H NMR analysis was operated on a Bruker instrument (400MHz-AVANCE III) at room temperature. FTIR were carried out by a Nicolet 6700 spectrophotometer by use of KBr. Thermogravimetric analysis (TGA) was conducted with a TGA/DSC instrument (Mettler-Toledo) under nitrogen protection at a heating rate of 10°C min^{-1} from 50 to 600°C. Melting temperatures (T_m) were recorded with differential scanning calorimetry (DSC) at a heating rate of 20°C min^{-1} from 25 to 300°C. $T_{\text{-10wt\%}}$ (temperatures at 10% weight loss), T_m, ^{1}H NMR and FTIR results were listed below.

BTA-nPr ($C_{18}H_{27}N_3O_3$): ^{1}H NMR(400 MHz, DMSO-d_6, δ): 0.88 (t, J = 7.4 Hz, 3H; CH_3,), 1.53 (m, 2H; CH_2), 3.23 (q, J = 6.5 Hz, 2H; CH_2), 8.34 (s, H; Ar-H), 8.65 (t, J = 5.7 Hz, H; NH); IR (KBr): v = 3327 (N–H), 3059 (C–H arom.), 2955 and 2871 (C–H aliph.), 1640 (C═O), 1533 (N–H deform.); T_m: 283 °C; $T_{\text{-10wt\%}}$: 339°C.

BTA-nBu ($C_{21}H_{33}N_3O_3$): ^{1}H NMR (400 MHz, $CDCl_3$, δ): 0.96 (t, J = 7.4 Hz, 3H; CH_3), 1.40 (m, 2H; CH_2), 1.61 (m, 2H; CH_2), 3.47 (m, 2H; CH_2), 6.67 (t, J = 5.0 Hz, H; NH), 8.24 (s, H; Ar-H); IR (KBr): v = 3235 (N–H), 3073 (C–H arom.), 2959 and 2873 (C–H aliph.), 1640 (C═O), 1561 (N–H deform.); T_m: 239°C; $T_{\text{-10wt\%}}$: 364°C.

BTA-nAm ($C_{24}H_{39}N_3O_3$): ^{1}H NMR (400 MHz, $CDCl_3$, δ): 0.92(t, J = 7.0 Hz, 3H; CH_3), 1.36 (m, 4H; CH_2), 1.62 (m, 2H; CH_2), 3.46 (m,2H; CH_2), 6.47 (t, J = 5.0 Hz, H; NH), 8.32 (s, H; Ar-H); IR (KBr): v = 3254 (N–H), 3076 (C–H arom.), 2930 and 2865 (C–H aliph.), 1643 (C═O), 1547 (N–H deform.); T_m: 219°C; $T_{\text{-10wt\%}}$: 350°C.

BTA-nHe ($C_{27}H_{45}N_3O_3$): ^{1}H NMR (400 MHz, $CDCl_3$, δ): 0.90(t, J = 7.0 Hz, 3H; CH_3), 1.32 (m, 6H; CH_2), 1.60 (m, 2H; CH_2), 3.42 (m, 2H; CH_2), 6.91 (t, J = 5.0 Hz, H; NH), 8.18 (s, H; Ar-H); IR (KBr): v = 3248 (N–H), 3076 (C–H arom.), 2929 and 2858 (C–H aliph.), 1636 (C═O), 1558 (N–H deform.); T_m: 209°C; $T_{\text{-10wt\%}}$: 384°C.

BTA-nOc ($C_{33}H_{57}N_3O_3$): ^{1}H NMR (400 MHz, $CDCl_3$, δ): 0.87 (t, J = 7.0 Hz, 3H; CH_3), 1.26 (m,10H; CH_2), 1.60 (m, 2H; CH_2), 3.44 (m, 2H; CH_2), 6.69 (t, J = 5.0 Hz, H; NH), 8.28 (s, H; Ar-H); IR (KBr): v = 3307 (N–H), 3076 (C–H arom.), 2926 and 2855 (C–H aliph.), 1645 (C═O), 1536 (N–H deform.); T_m: 208°C; $T_{\text{-10wt\%}}$: 387°C.

Sample Preparation

PLA and BTA-Rs were dried in a vacuum oven at 75°C for 12 h to remove residual water and then mixed at 175°C by a laboratory-scale conical twin-screw extruder (SJSZ-10A). The rotation speed and cycle time were set at 40 rpm and 5 min. The

obtained PLA/BTA-R was marked as PLA/BTA-R Φ, where Φ is the weight percentage of BTA-R.

Measurements

DSC. The nonisothermal and isothermal crystallization of PLA/BTA-R was studied by using a differential scanning calorimeter (Mettler-Toledo DSC). The measurements were conducted under nitrogen atmosphere. ~7 mg PLA/BTA-R samples were sealed in an aluminum pan, heated to 200°C and kept for 5 min to eliminate the thermal history. Nonisothermal and isothermal crystallization respectively proceeded by use of the samples. For the nonisothermal melt-crystallizations, samples were cooled to 25°C at 5 or 10°C min^{-1} and then heated to 200°C at 10°C min^{-1}. For the measurement of the nonisothermal cold-crystallization from the glassy state, the samples were quickly cooled to 25°C at −500°C min^{-1} from the melt and then heated to 200°C at 10°C min^{-1}. For the isothermal crystallization, the samples were cooled to the desired crystallization temperature at 50°C min^{-1} and kept until the isothermal crystallization was complete.

The measurement of nucleation efficiency (NE)[39]: For self-nucleation experiment, PLA was heated at 200°C min^{-1} to 200°C, and kept for 5 min to eliminate the thermal history, then cooled at 5°C min^{-1} to 80°C for the purpose of determining the crystallization peak temperature inherent to PLA in the absence of pre-existing nuclei (T_c^{min}), and heated at 200°C min^{-1} to the temperature with partial melting zone of PLA for another 5 min to create some PLA self-nucleated sites. The PLA sample was then cooled to 80°C at 5°C min^{-1} and the crystallization peak temperature of self-nucleated PLA was determined. The highest acquirable crystallization peak temperature from self-nucleated PLA melts was defined as T_c^{max}. For nucleation efficiency experiment, the samples were heated at 200°C min^{-1} to 183°C, and kept for 5 min, then cooled at 5°C min^{-1} to 80°C. The crystallization peak temperature (T_c) of samples was determined to estimate the NE.

The crystallinity (X_c) of samples was evaluated using eq. (1)

$$X_c = \frac{\Delta H_m}{(1-\Phi)\Delta H_m^*} \times 100\% \quad (1)$$

where $\triangle H_m$ is the measured endothermic enthalpy of melting, Φ is the weight fraction of BTA-nBu in the sample, and ΔH_m^* (the theoretical melting enthalpy of 100% crystalline PLA) was taken to be 93.6 J g^{-1}.[8]

WAXD. Wide-angle X-ray diffraction (WAXD) analysis was performed on a D8 Advance diffractometer (Bruker AXS) with a Cu Kα radiation (λ_x = 0.154 nm). The equipment was operated at 40 kV and 40 mA under ambient temperature. The scan range was between 5° and 40° with the rate of 3.5° min^{-1}.

POM. The PLA spherulites prepared by isothermal crystallization were observed with a polarized optical microscope (POM, Olympus BX51). The samples of pure PLA and PLA/BTA-nBu0.8 were located between two glass slides and heated to 200°C for 3 min. Then the sample was quickly cooled to the desired temperature for isothermal crystallization. The temperature was controlled by a hot stage (Linkam TH-600 PM).

RESULTS AND DISCUSSION

Comparison of BTA-R Nucleating Agents

The DSC thermograms of the nonisothermal melt-crystallization and subsequent heating scan for PLA with and without 1 wt % BTA-R derivatives are shown in Figure 2. The thermal parameters of PLA including of melt-crystallization temperature (T_{mc}), melt-crystallization enthalpy ($\triangle H_{mc}$), cold-crystallization temperature (T_{cc}), cold-crystallization enthalpy ($\triangle H_{cc}$), melting temperature (T_m), melt enthalpy ($\triangle H_m$), crystallinity (X_c), are summarized in Table I. The values of T_{mc} and $\triangle H_{mc}$ are obtained during the cooling process, and those of T_{cc}, $\triangle H_{cc}$, T_m, and $\triangle H_m$ are measured during the subsequent heating process. As shown in Figure 2, no melt-crystallization peak is detected for pure PLA in the cooling scan [Figure 2(a)] and a cold-crystallization peak is observed around 131°C in subsequent heating scan [Figure 2(b)]. It indicates the crystallization rate of pure PLA is slow. With addition of 1 wt % BTA-nOc or BTA-nHe, there is still no obvious melt-crystallization peak in the cooling scan curves [Figure 2(a)]. However, during the subsequent heating scan, the cold-crystallization peak appears at lower

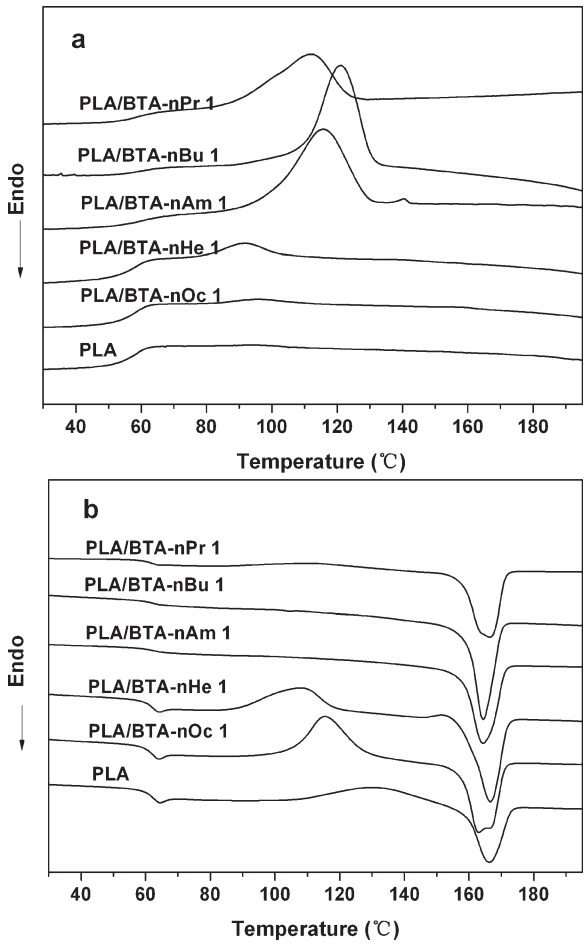

Figure 2. DSC thermograms of pure PLA and PLA/BTA-Rs: (a) nonisothermal melt-crystallization at cooling rate of 5°C min^{-1} and (b) subsequent heating scans at heating rate of 10°C min^{-1}.

Table I. Thermal Data of PLA with and Without BTA-Rs Obtained from Nonisothermal Melt-Crystallization and Subsequent Heating Scan

Sample	T_{mc} (°C)	ΔH_{mc} (J g^{-1})	T_{cc} (°C)	ΔH_{cc} (J g^{-1})	T_m (°C)	ΔH_m (J g^{-1})	X_c (%)
pure PLA	-	-	131	24.0	166	24.5	26.2
PLA/BTA-nPr 1	112	23.5	112	6.0	166	33.5	35.7
PLA/BTA-nBu 1	119	37.5	107	1.5	164	40.0	42.8
PLA/BTA-nAm 1	116	35.9	103	1.1	164	39.7	42.5
PLA/BTA-nHe 1	96	6.3	108	28.3	166	36.8	38.2
PLA/BTA-nOc 1	92	2.4	115	34.3	163	35.8	39.3

temperature as shown in Figure 2(b). This indicates that BTA-nHe and BTA-nOc can promote PLA molecular chains to form ordered structures in the heating process. By use of BTA-nAm, BTA-nBu, and BTA-nPr in PLA, obvious melt-crystallization peak is exhibited [Figure 2(a)] and cold-crystallization peak nearly disperses in the following heating scan [Figure 2(b)]. It means that the crystallization of the blends is completely in the cooling process. By understanding the principle of the crystallization behavior of PLA, it can be deduced that the crystallization rate of PLA is enhanced by BTA-Rs. In comparison with using of other BTA-R nucleating agents, PLA/BTA-nBu exhibits the sharpest and narrowest melt-crystallization peak in the cooling scan [Figure 2(a)]. It also shows the highest T_{mc} (119°C) and the largest $\triangle H_{mc}$ (37.5 J g^{-1}). Therefore, BTA-nBu shows the most excellent nucleation ability for PLA. In terms of higher T_{mc} and $\triangle H_{mc}$, the nucleation effects decreases in the order of BTA-nBu > BTA-nAm > BTA-nPr > BTA-nHe > BTA-nOc. BTA-nBu is selected to investigate its effect on the crystallization of PLA in more detail.

Influence of BTA-nBu Content on the Nonisothermal Crystallization of PLA

Figure 3 shows the DSC curves of nonisothermal melt-crystallization and following heating scan for PLA with different contents of BTA-nBu. With BTA-nBu, PLA appears obvious crystallization peak in the cooling scan [Figure 3(a)]. Crystallization rate is decided by the content of BTA-nBu. Figure 3(a) clearly shows the increase of crystallization rate is produced by increasing the content of BTA-nBu from 0.5 to 0.8 wt %. However, when the loading of BTA-nBu is larger than 0.8 wt %, the melt-crystallization peak shifts to low temperature and becomes broad [Figure 3(a)]. It may be attributed to the restriction of movement of PLA molecular chains to form ordered structures by using high amount of BTA-nBu. Similar results were found in other systems, such as PLLA/OMMT nanocomposites and PLA/*N*,*N*′-bis(benzoyl) suberic acid dihydrazide systems.[27] In Figure 3, PLA with 0.8 wt % BTA-nBu exhibits the sharpest but narrowest crystallization peak in nonisothermal melt-crystallization process [Figure 3(a)] and no cold-crystallization peak in the following heating scan [Figure 3(b)]. It can be concluded that 0.8 wt % BTA-nBu produces the best nucleation efficiency.

Nonisothermal cold-crystallization behavior of amorphous regions of the samples is also evaluated. Figure 4 shows the DSC curves recorded in the heating process of neat and BTA-nBu nucleated PLAs quenched from the melt. As shown in Figure 4, cold-crystallization peak appears sharper at lower temperature after adding BTA-nBu in PLA, meaning that the addition of BTA-nBu can improve the crystallization rate of PLA. Additionally the cold-crystallization rate of PLA also depends on the content of BTA-nBu. The cold-crystallization peak becomes small with the amount of BTA-nBu increasing from 0.5 to 0.8 wt %. This is caused by the fast crystallization of PLA/BTA-nBu 0.8 blend during the quenching process. With addition of 0.8 wt % BTA-nBu, PLA shows the highest crystallization rate with the lowest T_{cc}.

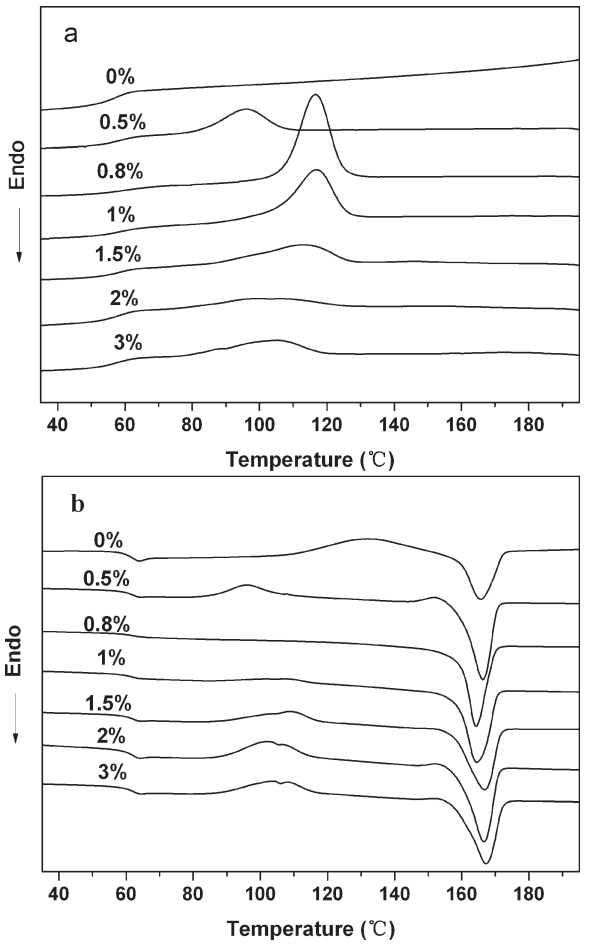

Figure 3. DSC thermograms of PLA with different contents of BTA-nBu: (a) nonisothermal melt-crystallization at cooling rate of 10°C min^{-1} and (b) subsequent heating scans at heating rate of 10°C min^{-1}.

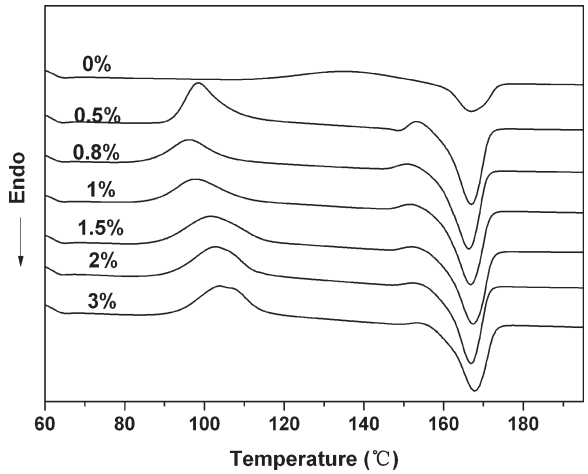

Figure 4. DSC thermograms of nonisothermal cold-crystallization from the glassy state of PLA with different contents of BTA-nBu at heating rate of 10°C min^{-1}.

In view of the difference in the thermal history of samples before crystallization, nonisothermal melt-crystallization and cold-crystallization from the glassy state are compared. The crystallization temperature and crystallinity in the two types of crystallization process are respectively plotted with the content of BTA-nBu in Figure 5. As seen from Figure 5, the values of

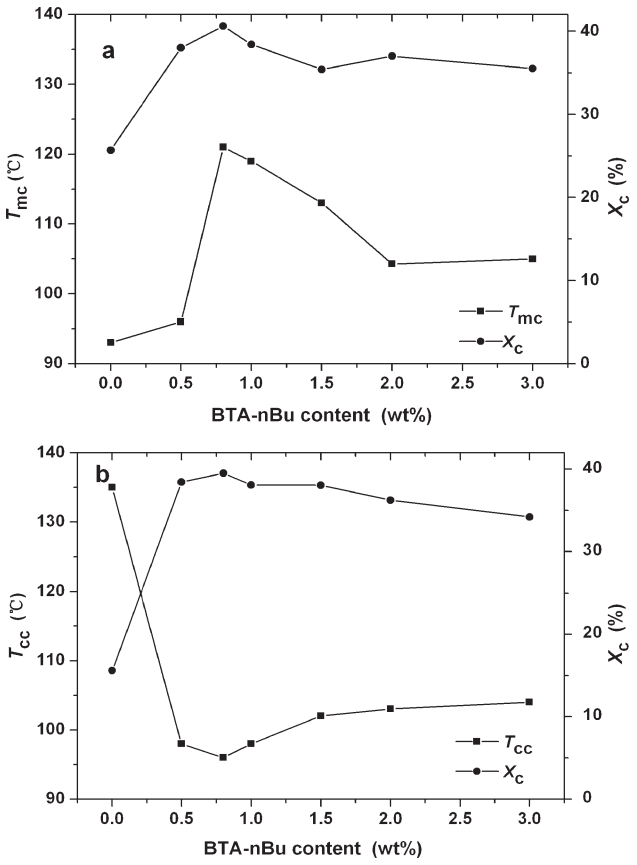

Figure 5. Crystallization temperature and crystallinity of PLA with different contents of BTA-nBu in melt-crystallization (a) and cold-crystallization from the glassy state (b).

Table II. NE of PLA with Different Contents of BTA-nBu

BTA-nBu content (wt %)	T_c (°C)	$\triangle H_c$ (J g^{-1})	NE (%)
0	97	0.6	0
0.5	104	23.8	27
0.8	121	30.1	91
1	119	28.8	83
1.5	118	24.6	79
2	106	19.0	35
3	106	15.3	35

T_{mc} are changed markedly with different BTA-nBu content, while the values of T_{cc} are not changed much. We consider that the difference in the variation tendency of the T_{mc} and T_{cc} can be explained by the classical crystallization theories. The crystallization via cooling from melt is controlled by the rate of nucleation, while the crystallization via heating from glassy state is controlled by both the nucleation rate and crystal growth rate. Thus, T_{mc} is more sensitive to the nucleation density than T_{cc}. Additionally, it is notable that PLA nucleated by 0.8 wt % BTA-nBu shows the largest crystallinity with highest T_{mc} [Figure

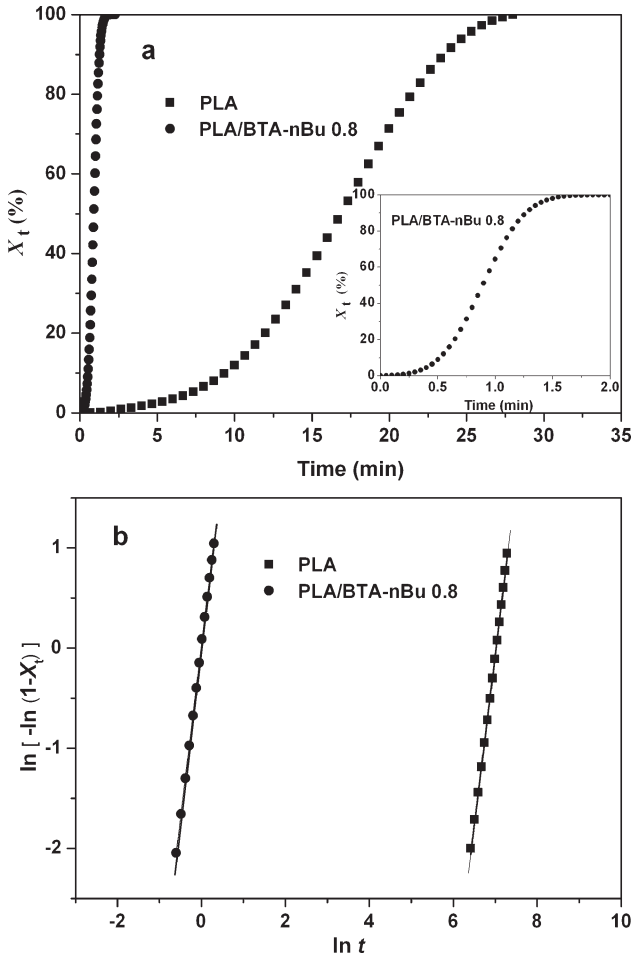

Figure 6. (a) The relative crystallization (X_t) as a function of crystallization time (t) and (b) Avrami plots of pure PLA and PLA/BTA-nBu 0.8 melt-crystallized isothermally at 120°C.

Table III. The Avrami Parameters of Pure PLA and PLA/BTA-nBu 0.8 Isothermally Crystallized at 120°C

Samples	$t_{1/2}$ (min)	n	k (min^{-n})
pure PLA	18	3.41	3.93×10^{-11}
PLA/BTA-nBu 0.8	0.8	3.46	1.02

5(a)] and lowest T_{cc} [Figure 5(b)], indicating that 0.8 wt % is the optimal amount of BTA-nBu to improve the crystallization rate of PLA. All the results in Figures 3–5 show 0.8 wt % BTA-nBu is the most suitable content for the improvement of crystallization rate of PLA.

Nucleation Efficiency of BTA-nBu

Fillon et al.[40] created a method to calculate the nucleation efficiency (NE) by considering the cooling process of polymer sample from the melt. Upon cooling, crystallization of polymer essentially happens at a particular temperature. With addition of an effective nucleating agent, a higher crystallization temperature (T_c) is usually observed because of the higher level of nucleation induced by the nucleating agent. The NE can be calculated from T_c using the following equation:

$$NE = \frac{T_c - T_c^{min}}{T_c^{\max} - T_c^{min}} \times 100 \qquad (2)$$

where T_c^{min} is the crystallization peak temperature of pure PLA without pre-existing nuclei, $T_c^{\max}$ is the highest achievable crystallization peak temperature from self-nucleated PLA melts, T_c is the crystallization peak temperature of samples. Self-nucleation is considered to be the ideal case for homopolymer crystallization due to an optimum dispersion of crystallites and the favorable interactions between the polymer melt and the polymer crystal fragments. Therefore, eq. (2) provides a way to directly compare the nucleating agent to the ideal self-nucleation case.[39] For the melt processed PLA at a cooling rate of 5°C min^{-1}, T_c^{min} and $T_c^{\max}$ are determined to be 97 and 123°C, respectively. The NE of PLA with different content BTA-nBu is calculated by eq. (2) and summarized in Table II. With 0.5 wt % BTA-nBu, the NE is only 27% due to its limited nucleation. It is reached up to 91% at addition of 0.8 wt % BTA-nBu in PLA. Excess BTA-nBu can lead to the decrease of NE. When loading of BTA-nBu is 2–3 wt %, the NE drops to 35%. Thus, 0.8 wt % BTA-nBu exhibits the highest NE suggesting an optimal amount for PLA crystallization. It has been reported that the NE of PLA with 6 wt % talc was 50% by Anderson.[39] Therefore, it is notable that the nucleation ability of the talc is lower than BTA-nBu crystallites even at higher weight fractions.

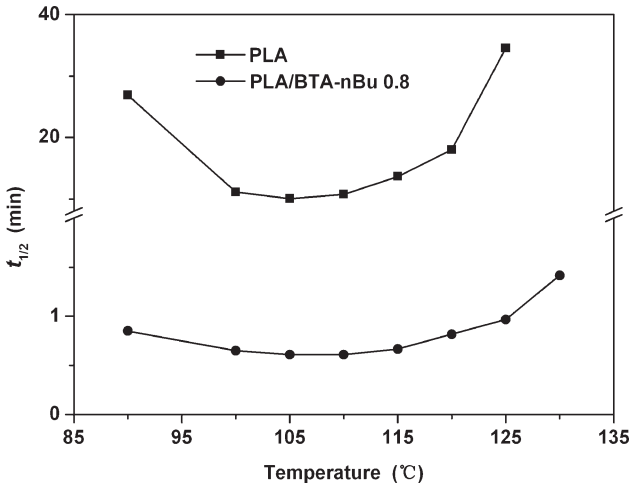

Figure 7. Crystallization half-time ($t_{1/2}$) of pure PLA and PLA/BTA-nBu 0.8 at different temperatures in isothermal melt-crystallization.

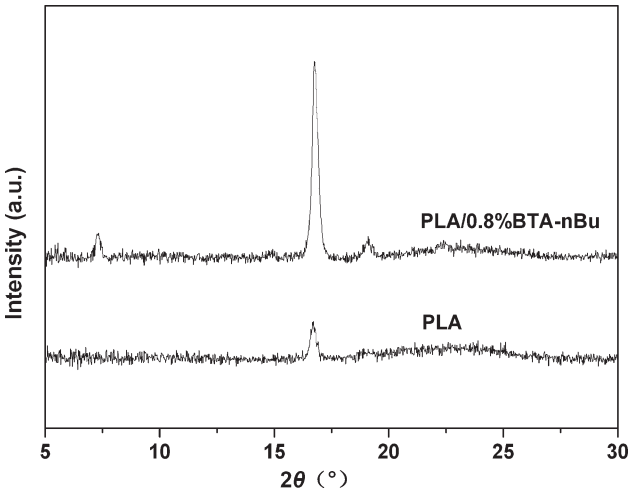

Figure 8. WAXD pattern of pure PLA and PLA/BTA-nBu 0.8 after treated by isothermal melt-crystallization at 105°C for 5 min.

Influence of BTA-nBu on the Isothermal Melt-Crystallization of PLA

In our experiment, isothermal melt-crystallization of PLA with and without 0.8 wt % BTA-nBu was further investigated in a wide temperature range from 90 to 130°C. To analyze the isothermal crystallization kinetics, the area, which is under the isothermal heat flow curve, was integrated to determine the relative crystallinity (X_t) of the samples as a function of crystallization time (t). The X_t can be calculated from the integrated

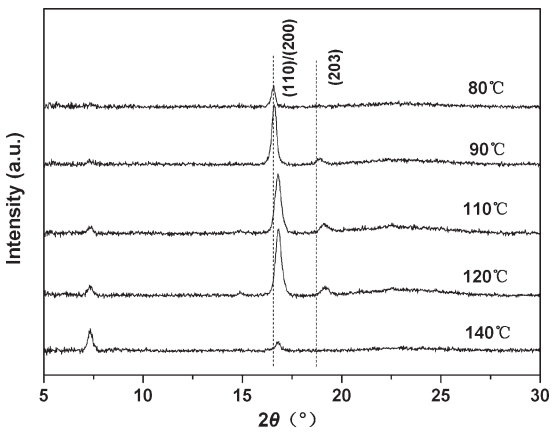

Figure 9. WAXD pattern of PLA/BTA-nBu 0.8 treated at different temperature in isothermal melt-crystallization for 5 min.

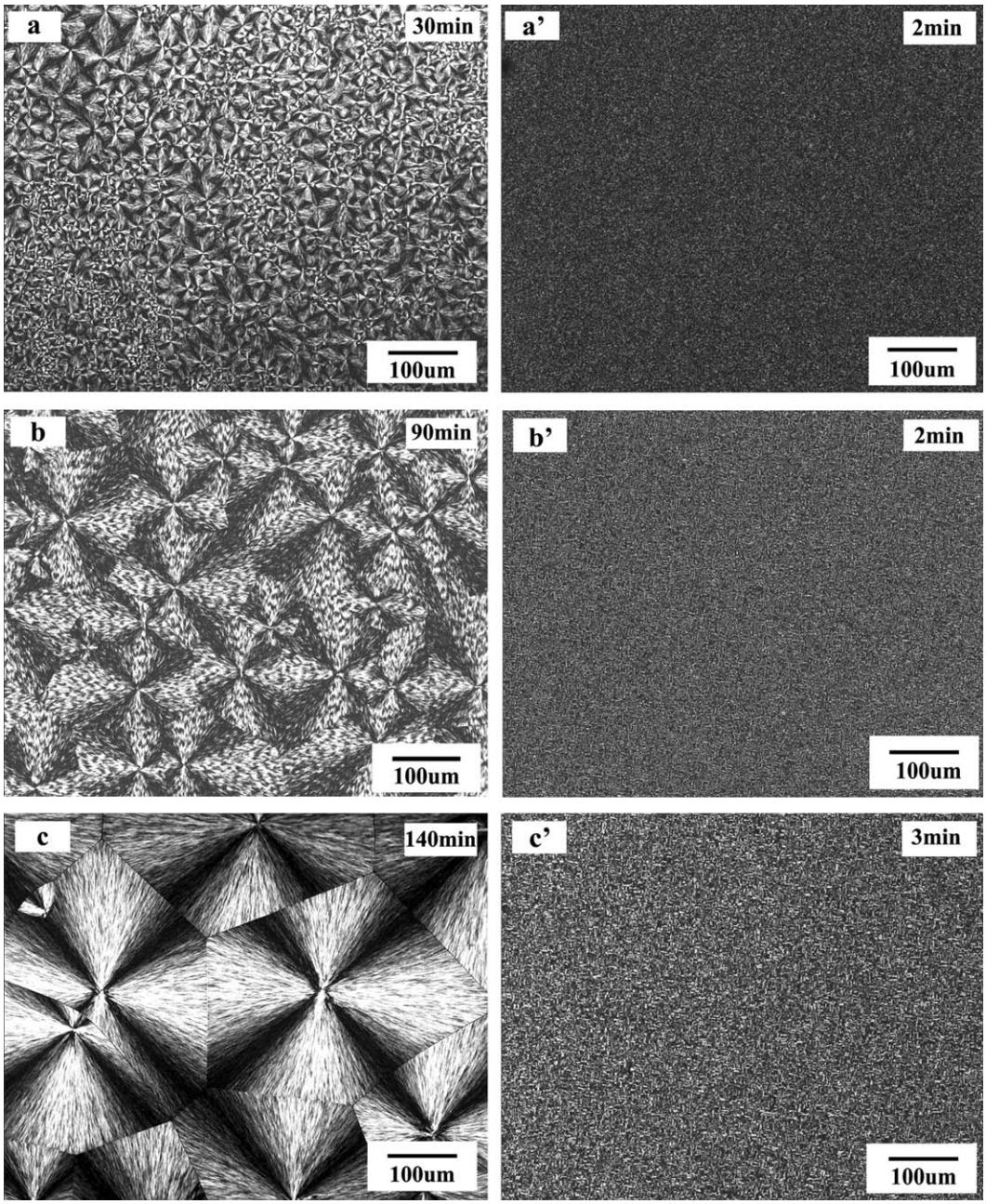

Figure 10. POM images of pure PLA (a–c) and PLA/BTA-nBu 0.8 (a′–c′) at crystallization temperature of 105°C (a, a′), 120°C (b, b′), and 130°C (c, c′).

area of the DSC curve from $t = 0$ to $t = t$, which is divided by the integrated area of the whole heat flow curve. Figure 6(a) shows the X_t as a function of t plots for the pure PLA and PLA/BTA-nBu 0.8 blend melt-crystallized isothermally at 120°C. The curves exhibit a sigmoid dependence on time. Pure PLA takes a long time (over 30 min) to complete crystallization. In contrast, the addition of 0.8 wt % BTA-nBu can effectively improve the crystallization rate of PLA, and the crystallization time is shortened to <2 min.

Isothermal melt-crystallization kinetics is analyzed by the well-known Avrami equation.[21,29,30] It describes that X_t develops with t as:

$$1 - X_t = \exp(-kt^n) \quad (3)$$

For convenience, the equation is often converted into the traditional linear form:

$$\ln[-\ln(1 - X_t)] = \ln k + n \ln t \quad (4)$$

where k is the overall kinetic rate constant that contains both the nucleation and growth rate parameters, and n is the Avrami exponent that depends on the mechanism of nucleation and the form of crystal growth.[29] Figure 6(b) shows the plots of $\ln[-\ln(1 - X_t)]$ versus $\ln t$ for the pure PLA and PLA/BTA-nBu 0.8 blend melt-crystallized isothermally at 120°C. The values of k and n can

be calculated from the slope and intercept of the fitted line, respectively. The parameters of isothermal crystallization kinetics calculated by employing Avrami equation are listed in Table III. The values of n are around 3.4, reflecting a three-dimensional crystal growth. The unit of k is min^{-n}, and n is not a constant at different isothermal crystallization temperature. Thus, it is not suitable to compare the total crystallization rate directly from k.[2,29]

The crystallization half-time ($t_{1/2}$), defined as the time when X_t reaches 50%, is also regarded as a very important crystallization kinetics parameter. It can be employed to characterize the crystallization rate directly. Figure 7 shows the $t_{1/2}$ plotted with crystallization temperature. Pure PLA shows large $t_{1/2}$ over 10 min. This phenomenon is attributed to the slow crystallization of PLA. After adding 0.8 wt % BTA-nBu, $t_{1/2}$ decreases significantly to around 1 min. The results indicate that the use of BTA-nBu improves the crystallization rate of PLA. As shown in Figure 7, the optimal temperature range for molding of PLA is between 100 and 110°C, between which one can obtain sufficiently high crystallinity. By using of 0.8 wt % BTA-nBu, the $t_{1/2}$ of PLA crystallized at 105°C is decreased from 10 to 0.6 min. Thus, it is reasonable to deduce that BTA-nBu can serve as a powerful nucleating agent for fast molding of PLA products in practical processing.

Figure 8 shows the WAXD patterns of pure PLA and PLA/BTA-nBu0.8 blend treated by the process of isothermal melt-crystallization at 105°C for 5 min. Pure PLA only shows a weak diffraction peak ($2\theta = 16.72°$). It is because of the low crystallinity of PLA. PLA/BTA-nBu 0.8 blend exhibits a strong diffraction at 16.76° and a weak peak at 19.13° related to the (200)/(110) and (203) planes, which are the characteristic peaks of PLA crystallite.[41] Another weak peak is observed at 7.32°, which is the crystallization of BTA-nBu. The results indicate that BTA-nBu can improve the crystallinity of PLA but cannot contribute to any change in crystalline structure. The crystalline structure of BTA-nBu nucleated PLA at different crystallization temperature is also studied. Figure 9 shows the WAXD results of PLA/BTA-nBu 0.8 blend annealed at crystallization temperature of 80, 90, 110, 120, and 140°C for 5 min. It is notable that the diffraction peaks of (110)/(200) and (203) planes shift to lower angle at low crystallization temperatures ($T_c < 110$°C). It can be attributed to the crystal transformation from α-form to disordered α-form (α-form) crystals of PLA. Similar results have been reported in the pure PLA.[41,42]

Spherulite Morphology

The spherulitic morphology of PLA/BTA-nBu was further analyzed with POM (Figure 10). It is obviously that the size of PLA spherulites becomes smaller in PLA/BTA-nBu blend than in pure PLA. With the temperature increase, the spherulites size becomes larger and larger in pure PLA, while it exhibits much the same size in PLA/BTA-nBu 0.8 blend. Moreover, the density of PLA spherulites is higher for BTA-nBu nucleated PLA. The results show that BTA-nBu can provide more nucleation sites for the crystallization of PLA as an efficient nucleating agent. With the increased nucleation density of PLA spherulites induced by BTA-nBu, the nonisothermal and isothermal crystallization of PLA can be enhanced, that is consistent with the previous results.

CONCLUSIONS

Five different substituted 1,3,5-trialkyl-benzenetricarboxylamides (BTA-R) were synthesized as the crystal nucleating agents for PLA. The crystallization of PLA is improved by using of BTA-Rs. Among these BTA-Rs, BTA-nBu shows the most excellent nucleation ability for PLA. By detailed evaluation of the nonisothermal melt-crystallization and cold-crystallization from the glassy state, the optimal weight fraction of BTA-nBu to improve the crystallization of PLA is found to be 0.8%. With 0.8 wt % BTA-nBu, the nucleation efficiency can reach up to 91%. The isothermal crystallization kinetics is analyzed by the Avrami model. The blend of PLA/BTA-nBu 0.8 exhibits a very short crystallization half-time around 1 min with a wide range of isothermal crystallization temperature. In addition, the results of isothermal WAXD analysis show that BTA-nBu can greatly improve the crystallization of PLA with no discernible effect on the crystalline structure. POM observation indicates BTA-nBu nucleated PLA exhibits smaller spherulites size and larger nucleation density than that of pure PLA. Thus, BTA-nBu is an efficient organic nucleating agent for improving the crystallization of PLA.

ACKNOWLEDGMENTS

The authors greatly thank the financial supports from the Ningbo Natural Science Foundation of China (No. 2011A610122), Ningbo Polymer Innovative Research Team (Grant No. 2009B21008) and Ningbo Key Lab of Polymer Materials (Grant No. 2010A22001).

AUTHOR CONTRIBUTIONS

Ting Wang: Nucleating agent design, synthesis and characterization, polymer crystallization testing and analysis, and drafting the artilce. Yong Yang: Polymer crystallization testing and analysis. Chuanzhi Zhang: Polymer crystallization testing and analysis. Zhaobin Tang: Polymer crystallization analysis. Haining Na: Revising the article critically. Jin Zhu: Promoter of the study and revising the article critically.

REFERENCES

1. Joo, M.; Auras, R.; Almenar, E. *Carbohydr. Polym.* **2011**, *86*, 1022.
2. Xing, Q.; Zhang, X.; Dong, X.; Liu, G.; Wang, D. *Polymer* **2012**, *53*, 2306.
3. Li, H.; Huneault, M. A. *Polymer* **2007**, *48*, 6855.
4. Kolstad, J. J. *J. Appl. Polym. Sci.* **1996**, *62*, 1079.
5. Garlotta, D. *J. Polym. Environ.* **2001**, *9*, 63.
6. Liao, R.; Yang, B.; Yu, W.; Zhou, C. *J. Appl. Polym. Sci.* **2007**, *104*, 310.
7. Harris, A. M.; Lee, E. C. *J. Appl. Polym. Sci.* **2008**, *107*, 2246.
8. Tang, Z.; Zhang, C.; Liu, X.; Zhu, J. *J. Appl. Polym. Sci.* **2012**, *125*, 1108.
9. Hassouna, F.; Raquez, J. M.; Addiego, F.; Toniazzo, V.; Dubois, P.; Ruch, D. *Eur. Polym. J.* **2012**, *48*, 404.

10. Hassouna, F.; Raquez, J.-M.; Addiego, F.; Dubois, P.; Toniazzo, V.; Ruch, D. *Eur. Polym. J.* **2011**, *47*, 2134.
11. Hu, Y.; Hu, Y. S.; Topolkaraev, V.; Hiltner, A.; Baer, E. *Polymer* **2003**, *44*, 5681.
12. Tábi, T.; Sajó, I. E.; Szabó, F.; Luyt, A. S.; Kovács, J. G. *Express. Polym. Lett.* **2010**, *4*, 659.
13. Wei, L.; Li, J.; Guo, S.; Xin, M.; Tian, Y.; Zhang, F. *J. Appl. Polym. Sci.* **2011**, *122*, 2708.
14. Carrasco, F.; Pagès, P.; Gámez-Pérez, J.; Santana, O. O.; Maspoch, M. L. *Polym. Degrad. Stabil.* **2010**, *95*, 116.
15. Yu, F.; Liu, T.; Zhao, X.; Yu, X.; Lu, A.; Wang, J. *J. Appl. Polym. Sci.* **2012**, *125*, E99.
16. Nam, J. Y.; Ray, S. S.; Okamoto, M. *Macromolecules* **2003**, *36*, 7126.
17. Su, Z.; Guo, W.; Liu, Y.; Li, Q.; Wu, C. *Polym. Bull.* **2009**, *62*, 629.
18. Tsuji, H.; Takai, H.; Fukuda, N.; Takikawa, H. *Macromol. Mater. Eng.* **2006**, *291*, 325.
19. Murariu, M.; Dasilvaferreira, A.; Degee, P.; Alexandre, M.; Dubois, P. *Polymer* **2007**, *48*, 2613.
20. Li, Y.; Chen, C.; Li, J.; Sun, X. S. *Polymer* **2011**, *52*, 2367.
21. Li, Y.; Chen, C.; Li, J.; Sun, X. S. *J. Appl. Polym. Sci.* **2012**, *124*, 2968.
22. Battegazzore, D.; Bocchini, S.; Frache, A. *Express Polym. Lett.* **2011**, *5*, 849.
23. Pan, P.; Liang, Z.; Cao, A.; Inoue, Y. *ACS Appl. Mater. Inter.* **2009**, *1*, 402.
24. Nam, J. Y.; Okamoto, M.; Okamoto, H.; Nakano, M.; Usuki, A.; Matsuda, M. *Polymer* **2006**, *47*, 1340.
25. Kawamoto, N.; Sakai, A.; Horikoshi, T.; Urushihara, T.; Tobita, E. *J. Appl. Polym. Sci.* **2007**, *103*, 244.
26. Kawamoto, N.; Sakai, A.; Horikoshi, T.; Urushihara, T.; Tobita, E. *J. Appl. Polym. Sci.* **2007**, *103*, 198.
27. Cai, Y.; Yan, S.; Yin, J.; Fan, Y.; Chen, X. *J. Appl. Polym. Sci.* **2011**, *121*, 1408.
28. Suryanegara, L.; Okumura, H.; Nakagaito, A. N.; Yano, H. *Cellulose* **2011**, *18*, 689.
29. Qiu, Z.; Li, Z. *Ind. Eng. Chem. Res.* **2011**, *50*, 12299.
30. Pan, P.; Yang, J.; Shan, G.; Bao, Y.; Weng, Z.; Inoue, Y. *Macromol. Mater. Eng.* **2012**, *97*, 670.
31. Abraham, F.; Ganzleben, S.; Hanft, D.; Smith, P.; Schmidt, H.-W. *Macromol. Chem. Phys.* **2010**, *211*, 171.
32. Blomenhofer, M.; Ganzleben, S.; Hanft, D.; Schmidt, H. W.; Kristiansen, M.; Smith, P.; Stoll, K.; Mader, D.; Hoffmann, K. *Macromolecules* **2005**, *38*, 3688.
33. Kristiansen, M.; Smith, P.; Chanzy, H.; Baerlocher, C.; Gramlich, V.; McCuskcr, L.; Weber, T.; Pattison, P.; Blomenhofer, M.; Schmidt, H. W. *Cryst. Growth Des.* **2009**, *9*, 2556.
34. Kristiansen, P. M.; Gress, A.; Smith, P.; Hanft, D.; Schmidt, H. W. *Polymer* **2006**, *47*, 249.
35. Wang, J.; Dou, Q.; Chen, X.; Li, D. *J. Polym. Sci. B Polym. Phys.* **2008**, *46*, 1067.
36. Bai, H.; Zhang, W.; Deng, H.; Zhang, Q.; Fu, Q. *Macromolecules* **2011**, *44*, 1233.
37. Song, P.; Wei, Z.; Liang, J.; Chen, G.; Zhang, W. *Polym. Eng. Sci.* **2012**, *52*, 1058.
38. Nakajima, H.; Takahashi, M.; Kimura, Y. *Macromol. Mater. Eng.* **2010**, *295*, 460.
39. Anderson, K. S.; Hillmyer, M. A. *Polymer* **2006**, *47*, 2030.
40. Fillon, B.; Thierry, A.; Lotz, B.; Wittmann, J. C. *J. Therm. Anal. Calorim.* **1994**, *42*, 721.
41. Pan, P.; Kai, W. H.; Zhu, B.; Dong, T.; Inoue, Y. *Macromolecules* **2008**, *41*, 4296.
42. Pan, P. J.; Kai, W. H.; Zhu, B; Dong, T.; Inoue, Y. *Macromolecules* **2007**, *40*, 6869.